

Stoichiometry of K⁺- and CO₃²⁻-Containing Apatites Prepared by the Hydrolysis of Octacalcium Phosphate

Ilse Y. Pieters,[†] Erna A. P. De Maeyer,^{‡,§} and Ronald M. H. Verbeek^{*,§}

Laboratory for Analytical Chemistry, University of Ghent, Krijgslaan 281-S12, B-9000 Ghent, Belgium, and Department of Dental Materials Science, University Hospital, University of Ghent, De Pintelaan 185, B-9000 Ghent, Belgium

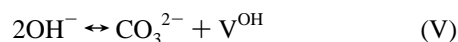
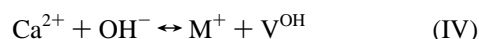
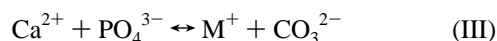
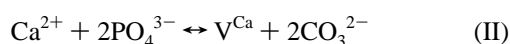
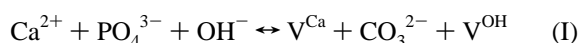
Received February 28, 1996[⊗]

In this study the composition of K⁺- and CO₃²⁻-containing hydroxyapatites (KCAp's) obtained by the hydrolysis of octacalcium phosphate (OCP), Ca₈(HPO₄)₂(PO₄)₄·5H₂O, was investigated as a function of the carbonate concentration c_{kc} and the molar K/CO₃ ratio R of the aqueous solution. OCP was hydrolyzed at 95 °C in K⁺- and CO₃²⁻-containing solutions with $2.5 \leq c_{\text{kc}} \text{ (mM)} \leq 100$ and $2 \leq R \leq 20$. Physical and chemical analyses showed that the precipitates were carbonated apatites with a carbonate content ranging from 2.5 to 5.5 wt %. The samples also contained a significant amount of monohydrogen phosphate (1.3–2.2 wt %) and an appreciable amount of water (3.5–5.5 wt %) after drying at 25 °C under vacuum. The chemical composition of the KCAp's can be explained by the occurrence of a main substitution mechanism [I: Ca²⁺ + PO₄³⁻ + OH⁻ ↔ V^{Ca} + CO₃²⁻ + V^{OH}] and a coupled K⁺ and CO₃²⁻ incorporation [III: Ca²⁺ + PO₄³⁻ ↔ K⁺ + CO₃²⁻] where V^X stands for a vacancy in the X sublattice. The relative contribution of mechanism III with respect to mechanism I increases with increasing c_{kc} and R .

Introduction

Calcium hydroxyapatite (HAp), Ca₁₀(PO₄)₆(OH)₂, is generally accepted as a prototype of apatite and is the most important inorganic compound of normal (tooth, bone), anomalous (plaque, renal stones), and pathological (atherosclerosis) calcifications in the higher vertebrates.¹ In these biological apatites, part of the lattice ions of HAp are substituted by ions such as CO₃²⁻, F⁻, Na⁺, and K⁺. In particular, the incorporation of carbonate has a considerable influence on the physical and physicochemical properties of the solid and hence on the mineralization, demineralization, and remineralization processes of these biominerals.^{1–3} Therefore it is of fundamental importance to know the mechanism(s) for carbonate incorporation in HAp.

According to De Maeyer *et al.*,⁴ the mechanisms proposed in literature can be related to six basic substitution mechanisms (I–VI) or a linear combination of some of them, where M stands



for an alkali metal and V^X represents a vacancy on a regular apatite lattice site occupied by X. The replacement of PO₄³⁻ ions by CO₃²⁻, resulting in so-called B-type CO₃²⁻, can occur in four different ways: mechanisms I, II, III, and VI. Substitution of the OH⁻ ion by CO₃²⁻, resulting in so-called A-type CO₃²⁻, occurs through one well established mechanism, V.^{1,5,6}

Mechanism IV represents an independent M⁺ incorporation and has been proposed by some investigators for M⁺ = Na⁺.^{7–10}

In previous studies M⁺- and CO₃²⁻-containing apatites (MCAp's) were prepared under homogeneous precipitation conditions by the hydrolysis of monetite (CaHPO₄) in M₂CO₃ solutions at 95 °C.^{8,10–12} On the basis of the chemical and physical characterization of the samples, mechanisms I and III were shown to be mainly responsible for M⁺ and/or CO₃²⁻ incorporation.

In this study octacalcium phosphate (OCP), Ca₈(HPO₄)₂(PO₄)₄·5H₂O, is used as a starting reagent for the synthesis of K⁺- and CO₃²⁻-containing apatites (KCAp's) under homogeneous precipitation conditions. The lower solubility of OCP enables the preparation of KCAp's in solutions with the same K₂CO₃ concentration, but with lower Ca and P concentrations when compared to the hydrolysis of monetite. In this way a further variation of the contribution of the substitution mechanisms becomes possible. Moreover, the use of OCP has also biological importance as this calcium phosphate is thought to be an essential precursor in the formation of biological apatites.^{13–18} The stoichiometry of the precipitated apatite is

(1) Driessens, F. C. M.; Verbeek, R. M. H. *Biomaterials*; CRC Press: Boca Raton, FL, 1990.

(2) McConnell, D. *Apatite*; Springer Verlag: Vienna, 1973.

(3) Verbeek, R. M. H. *Tooth development and caries*; CRC Press: Boca Raton, FL, 1986; Vol. I, 6.

(4) De Maeyer, E. A. P.; Verbeek, R. M. H. *Bull. Soc. Chim. Belg.* **1993**, *102* (9), 601.

(5) Elliott, J. C. *Calcif. Tissue Res.* **1969**, *3*, 293.

(6) Young, R. A.; Barlett, M. L.; Spooner, S.; Mackie, P. E.; Bonel, G. *J. Biol. Phys.* **1981**, *9*, 1.

(7) Nelson, D. G. A.; Featherstone, J. D. B. *Calcif. Tissue Int.* **1982**, *34*, S69.

(8) De Maeyer, E. A. P.; Verbeek, R. M. H.; Naessens, D. E. *Inorg. Chem.* **1994**, *33*, 5999.

(9) De Maeyer, E. A. P. Ph.D. Thesis, University of Ghent, Ghent, Belgium, 1992.

(10) Naessens, D. E. Ph.D. Thesis, University of Ghent, Ghent, Belgium, 1992.

(11) De Maeyer, E. A. P.; Verbeek, R. M. H.; Naessens, D. E. *Inorg. Chem.* **1993**, *32*, 5709.

(12) De Maeyer, E. A. P.; Verbeek, R. M. H.; Pieters, I. Y. *Inorg. Chem.* **1996**, *35*, 857.

(13) Brown, W. E.; Smith, J. P.; Lehr, J. R.; Frazier A. W. *Nature* **1962**, *196*, 1048.

* To whom correspondence and reprint requests should be addressed.

[†] Laboratory for Analytical Chemistry, University of Ghent.

[‡] Senior Research Assistant of the NFSR (Belgium).

[§] University Hospital, University of Ghent.

[⊗] Abstract published in *Advance ACS Abstracts*, August 1, 1996.

Table 1. Chemical Composition (Weight Percent)^a and Total Mass Balance % Σ of the Precipitates Dried at 25 °C

sample	c_{kc}^b (M)	R^c	% Ca	% PO ₄	% HPO ₄	% CO ₃	% K	% OH	% Σ
A2a	0.0025	2	37.81	51.45	1.59 ± 0.27	2.40	0.169	2.60 ± 0.10	96.02 ± 0.16
A2b		2	38.10	51.79	1.57 ± 0.27	2.54	0.158	2.58 ± 0.10	96.74 ± 0.16
A5		5	37.91	51.36	1.78 ± 0.27	2.62	0.189	2.54 ± 0.10	96.40 ± 0.16
A10		10	38.08	52.13	1.38 ± 0.27	2.55	0.230	2.49 ± 0.10	96.86 ± 0.16
A15		15	37.91	51.54	1.44 ± 0.27	2.77	0.267	2.53 ± 0.10	96.46 ± 0.16
A20		20	37.77	51.48	1.37 ± 0.27	2.78	0.243	2.44 ± 0.10	96.08 ± 0.16
B2	0.005	2	37.59	50.68	1.59 ± 0.26	3.23	0.286	2.41 ± 0.10	95.79 ± 0.16
B5		5	37.87	50.99	1.52 ± 0.27	3.51	0.317	2.36 ± 0.11	96.57 ± 0.16
B10		10	37.82	50.99	1.35 ± 0.27	3.49	0.357	2.40 ± 0.11	96.41 ± 0.16
B15		15	37.87	50.71	1.52 ± 0.26	3.60	0.434	2.50 ± 0.11	96.63 ± 0.16
B20		20	37.67	50.47	1.62 ± 0.26	3.58	0.420	2.44 ± 0.11	96.20 ± 0.16
C2A	0.010	2	37.56	50.38	1.35 ± 0.26	3.97	0.402	2.27 ± 0.11	95.93 ± 0.16
C2B		2	37.59	50.22	1.55 ± 0.26	3.84	0.365	2.35 ± 0.11	95.92 ± 0.16
C5		5	37.63	50.22	1.66 ± 0.26	3.92	0.430	2.34 ± 0.11	96.20 ± 0.16
C10		10	37.48	49.83	1.69 ± 0.26	4.25	0.487	2.25 ± 0.11	95.99 ± 0.16
C15		15	37.55	49.70	1.56 ± 0.26	4.38	0.571	2.39 ± 0.11	96.15 ± 0.16
C20		20	37.34	49.61	1.50 ± 0.26	4.45	0.534	2.22 ± 0.11	95.65 ± 0.16
D2	0.025	2	37.13	49.03	1.76 ± 0.26	4.71	0.574	2.12 ± 0.11	95.32 ± 0.16
D5		5	37.09	49.15	1.65 ± 0.26	4.87	0.641	2.01 ± 0.11	95.41 ± 0.16
D10		10	37.10	48.84	1.56 ± 0.26	5.08	0.753	2.15 ± 0.11	95.48 ± 0.16
D15		15	37.02	48.75	1.63 ± 0.26	5.24	0.762	2.00 ± 0.11	95.40 ± 0.16
E2a	0.050	2	36.79	48.42	1.82 ± 0.26	4.94	0.748	2.09 ± 0.11	94.81 ± 0.16
E2b		2	36.95	48.63	2.03 ± 0.26	4.95	0.722	2.01 ± 0.11	95.33 ± 0.16
E5		5	36.93	48.38	1.94 ± 0.25	5.40	0.835	1.97 ± 0.11	95.45 ± 0.16
E10		10	36.64	47.74	1.88 ± 0.25	5.64	1.096	2.06 ± 0.11	95.06 ± 0.16
F2	0.075	2	36.76	48.20	2.09 ± 0.25	5.22	0.797	1.96 ± 0.11	95.03 ± 0.16
G2a	0.100	2	36.79	48.02	2.08 ± 0.25	5.41	0.977	2.05 ± 0.11	95.33 ± 0.16
G2b		2	36.51	47.83	2.21 ± 0.25	5.27	0.917	1.92 ± 0.11	94.66 ± 0.16

^a The relative uncertainties on the amount of Ca, PO₄, CO₃, and K were determined as 0.2, 0.6, 2, and 2% respectively. ^b c_{kc} : carbonate concentration of the hydrolysis solution (mol L⁻¹). ^c R : molar K/CO₃ ratio of the hydrolysis solution.

determined as a function of the carbonate concentration and the molar K/CO₃ ratio of the aqueous solution.

Experimental Section

Preparation of KCAP. OCP was prepared by a controlled hydrolysis of brushite, CaHPO₄·2H₂O, as described elsewhere.¹⁹ Chemical analysis yielded 32.47 ± 0.06 wt % Ca and 18.78 ± 0.04 wt % P, resulting in a molar Ca/P ratio of 1.337 ± 0.004. (Theoretically: 32.63 wt % Ca, 18.91 wt % P, and Ca/P = 1.333). The KCAP's were prepared by the hydrolysis of 0.7 g/L OCP in a Teflon vessel at 95 °C and pH ≥ 9 in a K₂CO₃ solution (K₂CO₃·1.5H₂O, Merck, Suprapur) with a carbonate concentration c_{kc} ranging from 0.0025 to 0.1 M. The molar K/CO₃ ratio was varied from 2 to 20 by adding KNO₃ (Merck, Pro Analysis) to the solution. The suspension was continuously and thoroughly stirred. After 48 h the suspension was filtered, and the precipitates were thoroughly washed with hot distilled water (95 °C) and dried under vacuum until a constant weight was obtained.

Chemical Analysis. The calcium content of the precipitates was determined by a complexometric titration with ethylenediaminetetraacetic acid²⁰ using a Metrohm 665 Dosimat titrating unit. The total phosphorus content P was determined as orthophosphate with a Pye-Unicam PU8670 spectrophotometer using a slight modification of the method of Brabson *et al.*²¹ The potassium content was determined with a Dionex Ion Chromatograph 2110i. The method of Godinot *et*

*al.*²² was adapted for the determination of the carbonate content. The method consists of the determination of the carbon dioxide evolved from an acidified aqueous solution of the apatite using a Perkin-Elmer 8500 gas chromatograph. The HPO₄ content was determined by a modification of the method of Gee and Deitz.²³ The method is based on the pyrolysis of the samples at 400 °C for 1 h resulting in a conversion of HPO₄²⁻ into P₂O₇⁴⁻. The amount of pyrophosphate is then determined on the basis of the orthophosphate content before and after hydrolysis of the pyrolyzed sample in an acid solution. The uncertainty in the HPO₄ content was calculated by error propagation theory. In order to ensure that pH ≥ 9 during the synthesis, the pH of the synthesis solution was measured before and after hydrolysis with an Orion Ross Combination Glass Electrode (81-02 SC) and a Metrohm 605 pH-meter. For each measurement the electrode was calibrated at 95 °C with a phosphate buffer solution (pH = 6.89) and a disodiumtetraborate buffer solution (pH = 8.83).

Physical Analysis. X-ray powder diffraction patterns of the samples were recorded by step-scanning using a microprocessor controlled diffractometer system (Philips PW1830); Ni-filtered copper K α radiation was used with an automatic divergence slit PW1836 and a graphite monochromator. The dimensions a and c of the hexagonal unit cell of the apatites were calculated from the most intense and sharp reflections (usually $n > 20$) using a least-squares refinement program. A peak fit program was used to determine the exact position at maximum intensity and the full width at half-maximum (fwhm) of the diffraction peaks. IR spectra of the samples dispersed in CsBr tablets were recorded between 400 and 4000 cm⁻¹ with a resolution of 0.5 cm⁻¹ using a Galaxy Series FTIR-6030 spectrophotometer. The density of the samples was measured with a helium micropycnometer (Quantachrome Corp.) with an accuracy of 0.2%.

Results

Chemical Composition. The chemical composition of the precipitates is summarized in Table 1 as a function of the K₂-CO₃ concentration c_{kc} and the molar K/CO₃ ratio R of the

(14) Brown, W. E. *Clin. Orth. Rel. Res.* **1966**, *44*, 205.

(15) Brown, W. E.; Mathew, M.; Tung, M. S. *Progr. Crystal Growth Charact.* **1981**, *4*, 59.

(16) Hayek, E. *Klin. Wochenschr.* **1967**, *45*, 856.

(17) Weiss, M. P.; Voegel, J. C.; Frank, R. M. *J. Ultrastruct. Res.* **1981**, *76*, 286.

(18) Tomazic, B. B.; Brown, W. E.; Queral, L. A.; Sadovnik, M. *Atherosclerosis* **1988**, *69*, 5.

(19) Verbeeck, R. M. H.; Reyns, C. A. M. R.; Verbeeck, F.; Driessens, F. C. M. *J. Dent. Res.* **1985**, *64*, 716.

(20) Flaschka, H. A.; Barnard, A. J. Inorganic titrimetric analysis: Titrations with EDTA and related compounds. In *Comprehensive Analytical Chemistry*; Wilson C. L., Wilson D. W., Eds.; Elsevier Publ. Co: Amsterdam, 1960; Vol. IB.

(21) Brabson, J. A.; Dunn, R. L.; Epps, E. A.; Hoffman, W. M.; Jacob, K. D. *J. Assoc. Off. Agric. Chem.* **1958**, *41*, 517.

(22) Godinot, C.; Bonel, G.; Torres, L.; Mathieu, J. *Microchem. J.* **1984**, *29*, 92.

(23) Gee, A.; Deitz, V. R.; *J. Am. Chem. Soc.* **1955**, *77*, 2961.

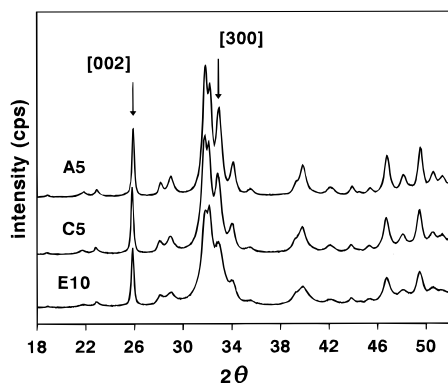


Figure 1. X-ray diffraction patterns of some representative samples with low (A5), medium (C5), and high (E10) carbonate content (intensity vs 2θ).

hydrolysis solution. The hydroxide content was calculated on the basis of the electroneutrality condition and the contents of Ca, PO₄, K, CO₃ and HPO₄ according to

$$\frac{\% \text{ OH}}{M_{\text{OH}}} = 2 \frac{\% \text{ Ca}}{M_{\text{Ca}}} + \frac{\% \text{ K}}{M_{\text{K}}} - 3 \frac{\% \text{ PO}_4}{M_{\text{PO}_4}} - 2 \frac{\% \text{ HPO}_4}{M_{\text{HPO}_4}} - 2 \frac{\% \text{ CO}_3}{M_{\text{CO}_3}} \quad (1)$$

M_X is the atomic or ionic mass of X. The total mass balance % Σ was calculated from

$$\% \Sigma = \% \text{ Ca} + \% \text{ K} + \% \text{ PO}_4 + \% \text{ HPO}_4 + \% \text{ CO}_3 + \% \text{ OH} \quad (2)$$

The errors on % OH and % Σ were estimated by error propagation theory.

Table 1 shows that the Ca and PO₄ contents of the samples decrease whereas the K and CO₃ contents increase with increasing c_{kc} for a given value of R . For a given carbonate concentration c_{kc} the K and CO₃ contents of the samples tend to increase with increasing molar K/CO₃ ratio R in the solution. The total mass balance is significantly lower than 100%, suggesting that the samples still contain 3.5 to 5.5% water. A regression analysis at the 95% confidence level shows that % Σ decreases and hence that the water content of the samples significantly increases with increasing CO₃ content according to

$$\% \Sigma = (97.87 \pm 0.53) - (0.50 \pm 0.13)[\% \text{ CO}_3] \quad (3)$$

It can be seen from Table 1 that the OH content of the samples slightly decreases with increasing c_{kc} for $c_{\text{kc}} < 0.025$ M, and becomes constant for $c_{\text{kc}} \geq 0.025$ M within experimental error. The HPO₄ content tends to increase with increasing c_{kc} .

Physical Analysis. Figure 1 represents the X-ray diffraction patterns of samples A5, C5, and E10, respectively with a low, medium, and high carbonate content. These samples are representative for the precipitates synthesized in the present study. All reflections can be attributed to the hexagonal crystal form of hydroxyapatite (ASTM-powder Diffraction File No. 9-432). In Figure 1 one can notice that the resolution of the diffraction peaks decreases and that their relative intensities change with increasing c_{kc} . The resolution and relative intensities however, are not affected by the molar K/CO₃ ratio R .

Figure 2 gives the fwhm (full width at half-maximum) of the [002] and [300] diffraction peaks calculated by a peak fit program as a function of the carbonate content of the precipitates. The relative uncertainties on fwhm[002] and [300] were calculated as 8 and 3%, respectively. The line broadenings of

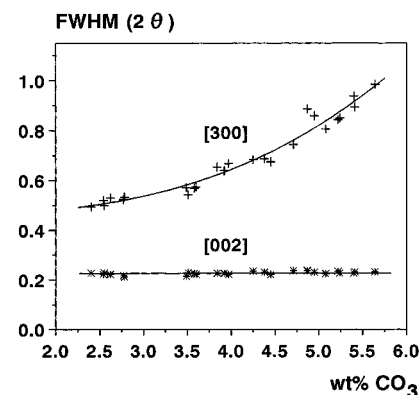


Figure 2. Full width at half-maximum (fwhm) of the [002] and [300] diffraction peak as a function of the carbonate content (wt %) of the samples after drying at 25 °C.

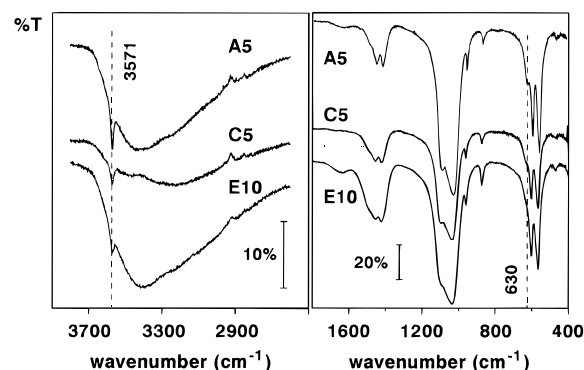


Figure 3. IR spectra of some representative precipitates with low (A5), medium (C5) and high (E10) carbonate content (% transmittance vs wavenumber).

the [002] and [300] diffraction peaks are chosen in the literature to study the degree of crystallinity (i.e. crystal size and/or lattice deformation and lattice defects) of carbonated apatites in the a - and c - axis direction respectively.²⁴⁻²⁶ Whereas the width of the [002] diffraction peak remains constant within the experimental error, the width of the [300] diffraction peak apparently increases with increasing carbonate content of the samples as is clearly illustrated with Figure 2. This is corroborated by a regression analysis which shows that on the 95% confidence level the following relationship holds:

$$\text{fwhm}[300] = (0.6998 \pm 0.1752) - (0.1771 \pm 0.0987)[\% \text{ CO}_3] + (0.0404 \pm 0.0131)[\% \text{ CO}_3]^2 \quad (4)$$

These observations are in agreement with the results of Trautz²⁷ and Chickerur *et al.*²⁸

The lattice parameters a and c of the precipitates vary from 0.9397 to 0.9435 nm and from 0.6877 to 0.6894 nm respectively. No correlation with the sample composition could be detected.

Figure 3 shows the IR spectra of samples A5, C5, and E10. Again, these spectra are representative for every precipitate in this study. The detected absorptions can be attributed to vibrations of HAp lattice ions. In the region 970–1100 cm⁻¹ the PO₄³⁻ absorptions are found. The intensity of the OH⁻

(24) Doi, Y.; Moriwaki, Y.; Aoba, T.; Takahashi, J.; Joshin, K. *Calcif. Tissue Int.* **1982**, *34*, 178.

(25) LeGeros, R. Z.; Trautz, O. R.; LeGeros, J. P.; Klein, E.; Shirra, W. P. *Science* **1967**, *155*, 1409.

(26) LeGeros, R. Z.; LeGeros, J. P.; Trautz, O. R.; Shirra, W. P. *Adv. X-ray Anal.* **1971**, *14*, 57.

(27) Trautz, O. R. *Ann. N. Y. Acad. Sci.* **1960**, *85*, 145.

(28) Chickerur, N. S.; Tung, M. S.; Brown, W. E. *Calcif. Tissue Int.* **1980**, *32*, 55.

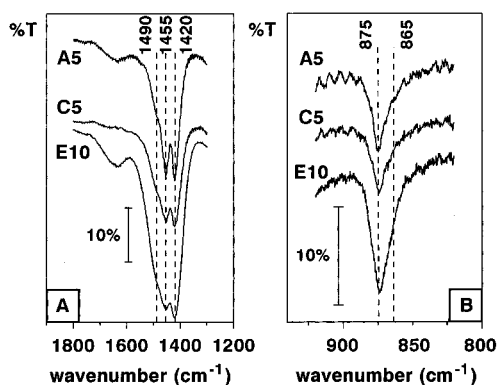


Figure 4. (A) Detail IR spectra of some representative precipitates in the carbonate absorption region between 820 and 920 cm^{-1} (% transmittance vs wavenumber). (B) Detail IR spectra of some representative precipitates in the carbonate absorption region between 1300 and 1800 cm^{-1} (% transmittance vs wavenumber).

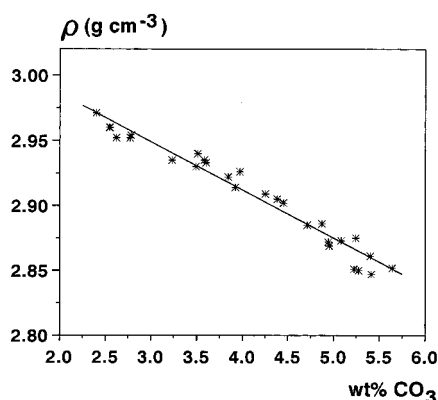


Figure 5. Density ρ (g cm^{-3}) of the samples as a function of their carbonate content (wt %) after drying at 25 $^{\circ}\text{C}$.

libration at 630 cm^{-1} and the stretching vibration at 3571 cm^{-1} decreases with increasing c_{kc} . This confirms the change of the OH content as a function of c_{kc} as shown by Table 1. The broad band between 2500 and 3700 cm^{-1} originates from water. Hence, one can conclude that the deviation of % Σ from 100% is mainly caused by a contamination with water. Parts A and B of Figure 4 give detail spectra of the same samples A5, C5, and E10, respectively between 820 and 920 cm^{-1} and between 1300 and 1800 cm^{-1} . In every spectrum an asymmetry at 865 cm^{-1} caused by the presence of HPO_4^{2-} is found.²⁹ This asymmetry was not observed in the MCAP's prepared by the hydrolysis of monetite.^{8,12} The CO_3^{2-} bending vibration is observed at 875 and the CO_3^{2-} stretching vibrations are observed at 1420, 1455, and 1490 cm^{-1} . For all the samples the absorption at 1490 cm^{-1} appears as a shoulder on the absorption at 1455 cm^{-1} . The intensity of the carbonate bands increases with increasing CO_3 content of the samples, which is in agreement with the results in Table 1.

The density of the samples as a function of the CO_3 content of the solid is presented in Figure 5. The decrease of the density ρ with increasing carbonate content can be attributed to the ionic substitutions. A weighted regression analysis shows that the relation between ρ and % CO_3 is linear and is on the 95% confidence level described by eq 5.

$$\rho(\text{g/cm}^3) = (3.060 \pm 0.011) - (0.037 \pm 0.003)[\% \text{CO}_3] \quad (5)$$

(29) Berry, E. E. *J. Inorg. Nucl. Chem.* **1967**, *29*, 317.

Discussion

The chemical and IR analyses reveal that the solids prepared in this study contain some HPO_4^{2-} (see Table 1). These HPO_4^{2-} ions most probably originate from unreacted OCP, as under the given preparation conditions ($\text{pH} \geq 9$ and $T = 95$ $^{\circ}\text{C}$) the incorporation of HPO_4^{2-} in the apatite lattice is very unlikely.³⁰ Moreover, according to Chickerur *et al.*²⁸ and Tomazic *et al.*³¹ the incomplete hydrolysis of OCP is caused by the inhibitory effect of carbonate on the transformation of OCP to apatite and results in a pronounced broadening of the [300] reflection, while the width of the [002] reflection is less affected. This is substantiated by the data in Figure 2 and by eq 4. However, incomplete hydrolysis does not lead to a separate OCP phase in the apatite structure, but to interlayered mixtures of OCP and apatite.^{14,15,32} This proposal is in agreement with the observed increase in water and HPO_4 contents in the solid with increasing carbonate content as shown by eq 3 and Table 1: due to carbonate inhibition on the hydrolysis of OCP, more hydrated OCP layers remain in the structure.

The lattice parameters a and c of the samples hardly correlate with the sample composition and, hence, with the CO_3 content. This can be explained by the relatively great error on the calculation of a and c caused by the relatively broad and less precisely localizable peaks in the diffraction patterns of the samples. However, as a is much more affected by CO_3^{2-} incorporation than c ,³³ one should still expect a significant variation of a with increasing carbonate content. That this variation is not observed could be caused by the simultaneous occurrence of A- and B-type CO_3^{2-} incorporation, as both types have an opposite effect on the lattice dimensions.³³ However, the occurrence of A-type CO_3^{2-} can not be demonstrated unambiguously by IR analysis. Although one could interpret the "shoulder" at 1490 cm^{-1} as arising from A-type CO_3^{2-} , the occurrence of CO_3^{2-} for OH^- substitution under the preparation conditions (aqueous system, high pH) used in the present study is not evident.^{34,35} Moreover, preliminary experiments showed that KCap's prepared by the hydrolysis of OCP at lower pH and with a comparable amount of CO_3^{2-} did clearly show the absorptions at 879 and at 1550 cm^{-1} , attributable to A-type CO_3^{2-} .^{36,37} This renders the presence of A-type CO_3^{2-} in the present samples very unlikely. Most probably, the shortening of a caused by the B-type CO_3^{2-} incorporation is mainly compensated for by the simultaneous incorporation of the larger K^+ ion.

When one wants to study the mechanisms for CO_3^{2-} incorporation in HAp, the absolute content of the unit cell of the samples must be known. This content can be calculated on the basis of the chemical composition of the samples, their density and their lattice dimensions. However, such a calculation can not be performed, because the precipitates still contain an appreciable amount of water which cannot be removed by drying at 25 $^{\circ}\text{C}$ under vacuum. Most probably, part of this

(30) De Maeyer, E. A. P.; Verbeeck, R. M. H.; Naessens, D. E. *J. Crystal Growth* **1994**, *135*, 539.

(31) Tomazic, B. B.; Mayer, I.; Brown, W. E. *J. Crystal Growth* **1991**, *108*, 670.

(32) Brown, W. E.; Schroeder, L. W.; Ferris, J. S. *J. Phys. Chem.* **1979**, *83*, 1385.

(33) LeGeros, R. Z.; Trautz, O. R.; Klein, E.; LeGeros, J. P. *Experientia* **1969**, *24*, 5.

(34) Vignoles, M.; Bonel, G.; Holcomb, D. W.; Young, R. A. *Calcif. Tissue Int.* **1988**, *43*, 33.

(35) Shimoda, S.; Aoba, T.; Moreno, E. C.; Miake, Y. *J. Dent. Res.* **1990**, *69*, 1731.

(36) Elliott, J. C. *Tooth Enamel*; Stack, M. V., Fearnhead, R. W., Eds.; Wright: Bristol, England, 1965.

(37) Bonel, G. *Ann. Chim.* **1972**, *7*, 65.

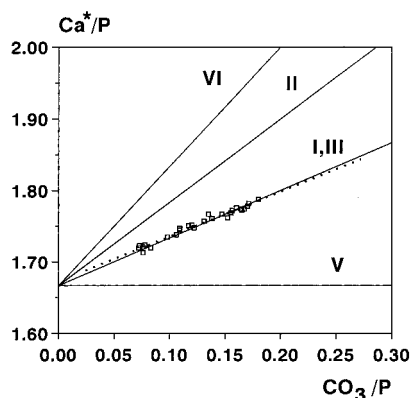
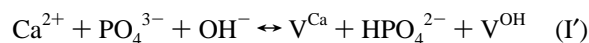


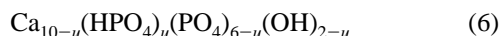
Figure 6. Molar Ca*/P ratio as a function of the molar CO₃/P ratio of the KCAp's (•••, experimental curve; —, theoretical curves according to mechanisms I–VI).

water is structural. It can either be associated with the OCP as discussed above or be present on vacant apatite lattice sites resulting from the incorporation of CO₃²⁻.¹¹ Another part may be nonstructural water, i.e. adsorbed on or occluded between the crystallites.^{8,11,38,39} Such water systematically causes an apparent decrease of the density as well as of the ionic contents and therefore should be removed from the samples. However, experiments showed that heating of the samples causes severe changes in the constitution of the samples (i.e. CO₃²⁻ loss and P₂O₇⁴⁻ formation). Consequently, the chemical composition and the density can not be corrected for this contamination.

Although the absolute content of the unit cell can not be deduced on the basis of the present results, indications for the occurrence of one or more of the mechanisms I–VI can be found on the basis of the relative contents of the lattice ions, presented by their molar Ca/P, CO₃/P and K/P ratios,¹¹ where P stands for the total molar phosphorus content of the samples (~PO₄³⁻ and HPO₄²⁻ content). In order to study the K⁺ and CO₃²⁻ incorporation in the apatite, the molar Ca/P ratio of the KCAp's, however, must be corrected for the presence of OCP. The stoichiometry of OCP-apatite mixtures can formally be accounted for by considering an apatite unit cell in which HPO₄²⁻ for PO₄³⁻ substitution took place according to mechanism I':



This substitution causes a vacancy on a calcium and hydroxide lattice site in HAp and results in the stoichiometry



where *u* stands for the number of HPO₄²⁻-ions per unit cell (*n*_{HPO₄}).

Hence, the molar (Ca + HPO₄)/P ratio, further referred to as Ca*/P, is the molar Ca/P ratio of the samples, corrected for the HPO₄²⁻ incorporation according to mechanism I'. Figure 6 gives the molar Ca*/P ratio as a function of the CO₃/P ratio. A regression analysis shows that the relation between the two variables, as represented by the dotted line in the figure, is linear and on the 95% confidence level described by eq 7. The full

$$[\text{Ca}^*/\text{P}] = (1.673 \pm 0.006) + (0.632 \pm 0.043)[\text{CO}_3/\text{P}] \quad (\text{7})$$

lines in Figure 6 represent the relations between Ca/P and CO₃/P that can be expected on the basis of the substitution mechanisms

(38) LeGeros, R. Z.; Bonel, G.; Legros, R. *Calcif. Tissue Res.* **1978**, *26*, 111.

(39) Davidson, C. L.; Arends, J. *Caries Res.* **1977**, *11*, 313.

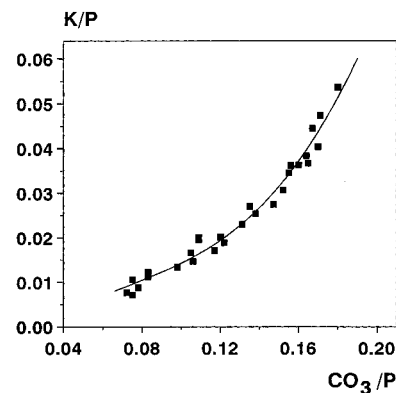


Figure 7. Molar K/P ratio as a function of the molar CO₃/P ratio of the samples.

I–VI. The experimental curve given by eq 7 coincides with the theoretical curve for substitution mechanisms I and III i.e. for CO₃/P = 0, Ca*/P reaches within the experimental error the molar Ca/P ratio of pure HAp (1.667). Moreover, the slope of the curve given by eq 7 equals the value 0.666 that can be expected on the basis of the substitution mechanisms I and III. Because for every sample the molar CO₃/P ratio exceeds the molar K/P ratio and the K/P and CO₃/P molar ratios are positively correlated as shown in Figure 7, it is then clear that the coupled K⁺–CO₃²⁻ incorporation (III) as well as the independent CO₃²⁻ incorporation (I) are the two mechanisms which contribute to the stoichiometry of the KCAp's, according to formula 8, where *x* and *y* represent the contributions



respectively of mechanisms I and III. The observed complexity in the carbonate absorption region in the IR spectra can then be ascribed to the occurrence of the two substitution mechanisms I and III leading to a different surrounding of CO₃²⁻ in the apatite lattice¹² and/or the presence of remaining hydrated OCP layers which may cause H₂O–CO₃²⁻ interactions.

If only mechanisms I and III account for the CO₃²⁻ incorporation in the apatite the phosphate sublattice must always be fully occupied in the apatite unit cell. In fact, on the basis of the stoichiometry of the mechanisms I and III the sum of the number of orthophosphate ions per apatite unit cell *n*_{PO₄} and the number of carbonate ions per apatite unit cell *n*_{CO₃} is always equal to 6. Moreover, in the OCP unit cells the sum of the number of orthophosphate ions *n*_{PO₄} and the number of mono-hydrogenphosphate ions *n*_{HPO₄} is also equal to 6 (see mechanism I'). Consequently, the following equation holds for interlayered mixtures of apatite and OCP:

$$n_p + n_{\text{CO}_3} = 6 \quad (\text{9})$$

Here

$$n_p = n_{\text{PO}_4} + n_{\text{HPO}_4} \quad (\text{10})$$

On the basis of eq 9 and the chemical composition of the samples it is possible to calculate the mean content of the unit cell of the KCAp's. The number of X ions per unit cell is given by eq 11, % X represents the content of X (wt %) and *M*_X its

$$n_x = \frac{6}{\frac{\% \text{P}}{M_p} + \frac{\% \text{CO}_3}{M_{\text{CO}_3}}} \left(\frac{\% \text{X}}{M_x} \right) \quad (\text{11})$$

ionic mass. The results of this calculation are given in Table

Table 2. Unit Cell Content of the Precipitates Calculated from the Data in Table 1 and by Means of eq 11

sample	n_{Ca}	n_{PO_4}	n_{CO_3}	$n_K = y$	$n_{HPO_4} = u$	n_{OH}	x
A2a	9.460 ± 0.029	5.433 ± 0.029	0.401 ± 0.008	0.043 ± 0.001	0.166 ± 0.028	1.534 ± 0.069	0.358 ± 0.008
A2b	9.443 ± 0.029	5.417 ± 0.029	0.420 ± 0.008	0.040 ± 0.001	0.162 ± 0.028	1.506 ± 0.070	0.380 ± 0.008
A5	9.412 ± 0.029	5.381 ± 0.029	0.434 ± 0.008	0.049 ± 0.001	0.185 ± 0.028	1.485 ± 0.071	0.385 ± 0.008
A10	9.411 ± 0.029	5.437 ± 0.029	0.421 ± 0.008	0.059 ± 0.001	0.142 ± 0.028	1.450 ± 0.070	0.363 ± 0.008
A15	9.398 ± 0.029	5.392 ± 0.029	0.459 ± 0.009	0.068 ± 0.001	0.149 ± 0.028	1.476 ± 0.072	0.391 ± 0.009
A20	9.382 ± 0.029	5.397 ± 0.029	0.461 ± 0.009	0.062 ± 0.001	0.142 ± 0.028	1.431 ± 0.072	0.399 ± 0.009
B2	9.316 ± 0.030	5.301 ± 0.029	0.535 ± 0.010	0.073 ± 0.001	0.165 ± 0.027	1.406 ± 0.075	0.462 ± 0.010
B5	9.275 ± 0.031	5.270 ± 0.029	0.574 ± 0.010	0.080 ± 0.002	0.155 ± 0.027	1.359 ± 0.077	0.494 ± 0.010
B10	9.295 ± 0.031	5.289 ± 0.029	0.573 ± 0.010	0.090 ± 0.002	0.139 ± 0.027	1.364 ± 0.077	0.483 ± 0.011
B15	9.296 ± 0.031	5.254 ± 0.029	0.590 ± 0.011	0.109 ± 0.002	0.156 ± 0.027	1.449 ± 0.078	0.481 ± 0.011
B20	9.276 ± 0.031	5.245 ± 0.029	0.589 ± 0.011	0.106 ± 0.002	0.167 ± 0.027	1.415 ± 0.078	0.483 ± 0.011
C2a	9.208 ± 0.032	5.212 ± 0.029	0.650 ± 0.012	0.101 ± 0.002	0.138 ± 0.027	1.310 ± 0.080	0.549 ± 0.012
C2b	9.241 ± 0.031	5.210 ± 0.029	0.630 ± 0.011	0.092 ± 0.002	0.159 ± 0.027	1.363 ± 0.080	0.538 ± 0.011
C5	9.213 ± 0.032	5.189 ± 0.029	0.641 ± 0.012	0.108 ± 0.002	0.170 ± 0.027	1.350 ± 0.080	0.533 ± 0.012
C10	9.152 ± 0.032	5.135 ± 0.029	0.693 ± 0.012	0.122 ± 0.002	0.172 ± 0.027	1.296 ± 0.083	0.571 ± 0.013
C15	9.176 ± 0.033	5.126 ± 0.029	0.715 ± 0.013	0.143 ± 0.003	0.159 ± 0.026	1.373 ± 0.084	0.572 ± 0.013
C20	9.131 ± 0.033	5.120 ± 0.029	0.727 ± 0.013	0.134 ± 0.003	0.153 ± 0.026	1.281 ± 0.085	0.593 ± 0.013
D2	9.067 ± 0.033	5.052 ± 0.029	0.768 ± 0.013	0.144 ± 0.003	0.179 ± 0.026	1.274 ± 0.087	0.624 ± 0.014
D5	9.015 ± 0.034	5.042 ± 0.030	0.791 ± 0.014	0.160 ± 0.003	0.167 ± 0.026	1.151 ± 0.088	0.631 ± 0.014
D10	9.028 ± 0.034	5.016 ± 0.030	0.826 ± 0.014	0.188 ± 0.004	0.159 ± 0.026	1.231 ± 0.090	0.638 ± 0.015
D15	8.973 ± 0.035	4.987 ± 0.030	0.848 ± 0.015	0.189 ± 0.004	0.165 ± 0.026	1.145 ± 0.091	0.659 ± 0.015
E2	9.013 ± 0.034	5.006 ± 0.029	0.808 ± 0.014	0.188 ± 0.004	0.186 ± 0.026	1.205 ± 0.088	0.620 ± 0.015
E5	8.984 ± 0.034	4.990 ± 0.029	0.804 ± 0.014	0.180 ± 0.004	0.206 ± 0.026	1.154 ± 0.088	0.624 ± 0.014
E10	8.922 ± 0.035	4.933 ± 0.030	0.871 ± 0.015	0.207 ± 0.004	0.196 ± 0.026	1.122 ± 0.092	0.664 ± 0.016
E15	8.901 ± 0.036	4.894 ± 0.030	0.915 ± 0.016	0.273 ± 0.006	0.191 ± 0.026	1.176 ± 0.094	0.642 ± 0.017
F2	8.929 ± 0.035	4.941 ± 0.030	0.847 ± 0.015	0.198 ± 0.004	0.212 ± 0.026	1.120 ± 0.090	0.649 ± 0.015
G2a	8.920 ± 0.035	4.913 ± 0.030	0.876 ± 0.015	0.243 ± 0.005	0.211 ± 0.026	1.171 ± 0.092	0.633 ± 0.016
G2b	8.894 ± 0.035	4.918 ± 0.030	0.857 ± 0.015	0.229 ± 0.005	0.225 ± 0.026	1.103 ± 0.091	0.628 ± 0.015

2. The errors were estimated by means of error propagation theory. Table 2 shows that for every sample eq 12 holds,

$$n_{Ca} = 4 + n_{PO_4} \quad (12)$$

indicating that only mechanisms I, I', and III contribute to the stoichiometry of the unit cells of the precipitates. Neglecting the water content, their mean stoichiometry can be represented by formula 13. The contributions x , y , and u can be calculated



according to

$$x = n_{CO_3} - n_K \quad (14)$$

$$y = n_K \quad (15)$$

$$u = n_{HPO_4} \quad (16)$$

The results of this calculation are also summarized in Table 2.

A plot of x and y for KCAp's obtained by the hydrolysis of OCP and monetite¹² vs c_{kc} for $R = 2$ is shown in Figure 8. For the KCAp's prepared in this study, the contributions of both mechanisms I and III to the total CO_3^{2-} incorporation increase with increasing c_{kc} for $c_{kc} \leq 0.025M$. From $c_{kc} > 0.025M$, however, the contribution of mechanism I remains constant, while the coupled potassium-carbonate incorporation according to mechanism III still increases. The former is in agreement with the observed decrease in OH content of the samples with increasing c_{kc} for $c_{kc} \leq 0.025M$ as evidenced by Table 1 and the IR spectra, suggesting a substitution mechanism for carbonate involving OH^- ions. For higher values of c_{kc} , x and hence n_{OH} remain constant. Moreover, the variation of x and y with c_{kc} apparently explains the nonlinear increase of the molar K/P ratio as a function of the molar CO_3/P ratio in Figure 7. Figure 8 also illustrates that by taking OCP as starting reagent for the hydrolysis instead of monetite,¹² the contribution of the main substitution mechanism I (x) to the total carbonate incorporation

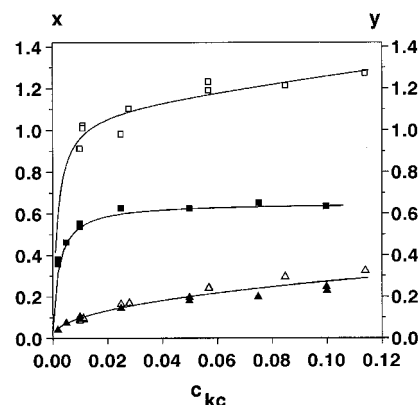


Figure 8. Contribution per unit cell of mechanisms I (x) and III (y) to the stoichiometry of the KCAp's prepared by the hydrolysis of OCP ($x = \blacksquare$, $y = \blacktriangle$) and monetite¹² ($x = \square$, $y = \triangle$) as a function of the carbonate concentration c_{kc} (M) in the hydrolysis solution for $R = 2$.

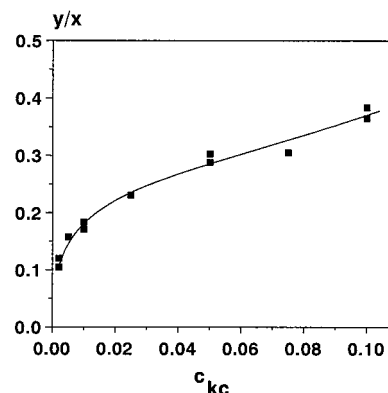


Figure 9. Ratio y/x of the contribution of mechanism III (y) and the contribution of mechanism I (x) to the total carbonate incorporation as a function of the carbonate concentration c_{kc} (M) in the hydrolysis solution for $R = 2$.

drastically decreases, whereas the contribution of mechanism III (y) hardly changes. Hence, hydrolysis of OCP results in KCAp's with a lower carbonate content, approaching that of biological apatites such as enamel and dentine.^{1,40}

Figure 9 illustrates that the ratio y/x increases with increasing c_{kc} , indicating that the relative contribution of mechanism III with respect to mechanism I to the total carbonate incorporation increases with increasing c_{kc} . This corroborates that both mechanisms are not intrinsically coupled.^{8,12}

From Table 2 it is seen that x tends to increase and that y increases with increasing R for a given value of c_{kc} . This indicates that an increase of the potassium concentration in the solution increases the driving force for carbonate incorporation. As could be expected, the relative increase in the contribution with increasing R is much more pronounced for mechanism III,

in which K⁺ is involved, than for the individual B-type CO₃²⁻ incorporation according to mechanism I.

Conclusions

KCAp's prepared by the hydrolysis of OCP under homogeneous precipitation conditions are to be considered as interlayered mixtures of OCP and carbonated apatite. The stoichiometry of the apatite layers in the KCAp's conforms to that of HAp in which the lattice ions are substituted by K⁺ and CO₃²⁻ according to the mechanisms [I: Ca²⁺ + PO₄³⁻ + OH⁻ ↔ V^{Ca} + CO₃²⁻ + V^{OH}] and [III: Ca²⁺ + PO₄³⁻ ↔ K⁺ + CO₃²⁻]. The results show that both mechanisms are not intrinsically coupled. Mechanism I is the main substitution mechanism, but the contribution of mechanism III increases with increasing c_{kc} and R .

(40) Moreno, E. C.; Aoba, T. *Calcif. Tissue Int.* **1991**, *49*, 6.